EVALUATION OF DIFFRACTION BEHIND A SEMI-INFINITE BREAKWATER IN THE SWAN WAVE MODEL

François Enet, Alphonse Nahon[1], Gerbrant van Vledder, David Hurdle
Alkyon Hydraulic Consultancy & Research, PO Box 248,
8300AE Emmeloord,
The Netherlands
Email: enet@alkyon.nl, nahon@alkyon.nl, vledder@alkyon.nl, hurdle@alkyon.nl

1 INTRODUCTION

Information on the penetration of waves behind breakwaters is important for the design of harbours and to assess the safety of mooring systems. Such information is usually obtained with numerical modelling. The numerical modelling has to take care of all processes affecting the waves as they approach and enter a harbour. In most cases harbours are located along a shallow coast where refraction and diffraction affect the penetration of waves into a harbour. For large harbour areas also local wave generation may play role.

The effects of refraction and local wave generation are easily accounted for with phase-averaged models. Examples of such models are the discrete spectral models WAM and SWAN (Booij et al., 1999). These models are not normally used to account for diffraction. Diffraction is usually computed with phase-resolving models, like Boussinesq (e.g., Borsboom et al., 2001) or mild-slope models (Berkhoff, 1972). Traditionally, phase-averaged models have been used to compute the wave conditions in the coastal zone and phase-resolving models have been used to determine the wave conditions in the harbour, if necessary coupling the models. A recent example of such a coupling is given in Groeneweg et al. (2004).

Phase-averaged models are more efficient than phase-resolving models. Therefore, several attempts have been made to include the effects of diffraction in spectral wave models (Rivero et al., 1997) and Holthuijsen et al., (2003). Recently, version 40.51 of the SWAN model was released (Holthuijsen et al., 2004). This version includes an approximation to diffraction according to the equations given in Holthuijsen et al. (2003).

Since the SWAN model is widely used in coastal engineering practice, we were interested in the applicability of diffraction in the SWAN model. The purposes of this paper are therefore:

- Test the implementation of diffraction in SWAN with an emphasis on numerical stability and guidelines for proper usages;
- Verify the diffraction approximation against an analytical solution;
- Assess the importance of diffraction for wind waves and for swell waves;
- Formulate guidelines for modelling diffraction with SWAN.

As a first step, we have investigated the performance of diffraction in SWAN for a simple situation; the semi-infinite breakwater in water of constant depth and omitting the growth by wind and dissipation by depth effects. The input wave conditions consisted of a narrow banded frequency spectrum with various amount of directional spreading.

[1] At Alkyon on internship from Matmeca, University of Bordeaux I, France, alphonse.nahon@etu.u-bordeaux1.fr

2. IMPLEMENTATION OF DIFFRACTION IN SWAN

The SWAN model uses the action balance to compute the evolution of the wave field in time and space. This equation is given by:

$$\frac{\partial N}{\partial t}+\frac{\partial\left(c_x N\right)}{\partial x}+\frac{\partial\left(c_y N\right)}{\partial y}+\frac{\partial\left(c_\sigma N\right)}{\partial \sigma}+\frac{\partial\left(c_\theta N\right)}{\partial \theta}=\frac{S}{\sigma} \tag{1}$$

Where the action density is defined as $N=N\left(\sigma,\theta\right)=E\left(\sigma,\theta\right)/\sigma$ with σ the relative frequency. The velocity c_σ is the propagation speed in frequency space and c_θ is the propagation speed due to refraction. The term S is the source term describing all the physical processes of growth, decay and redistribution of wave energy. In the case without diffraction the propagation velocities in x-y and spectral space are given by (Holthuijsen et al., 2003):

$$\vec{c}_g=\left(c_x,c_y\right)=\frac{\vec{\kappa}}{\kappa}\frac{\partial\sigma}{\partial k}+\vec{U} \tag{2}$$

$$c_\sigma=\frac{\partial\sigma}{\partial d}\left[\frac{\partial d}{\partial t}+\vec{U}\bullet\nabla d\right]-c_g\vec{\kappa}\bullet\frac{\partial\vec{U}}{\partial s} \tag{3}$$

$$c_\theta=-\left[c_g\left(\frac{1}{\kappa}\frac{\partial\kappa}{\partial m}\right)+\frac{\vec{\kappa}}{\kappa}\frac{\partial\vec{U}}{\partial m}\right] \tag{4}$$

In these equations $\vec{U}$ is the ambient current vector, d is depth and m a local coordinate perpendicular to the direction of wave propagation. In the absence of diffraction the separation parameter κ is equal to the wave number k.

If diffraction is accounted for, a correction term δ_E is added to the above propagation velocities. The equations then become:

$$\vec{C}_g=\vec{c}_g\left(1+\delta_E\right)^{1/2}+\vec{U} \tag{5}$$

$$c_\sigma=\frac{\partial\sigma}{\partial d}\left[\frac{\partial d}{\partial t}+\vec{U}\bullet\nabla d\right]-c_g\vec{\kappa}\bullet\frac{\partial\vec{U}}{\partial s}\left(1+\delta_E\right)^{1/2} \tag{6}$$

$$c_\theta=-\left[c_g\left(1+\delta_E\right)^{1/2}\left(\frac{1}{\kappa}\frac{\partial\kappa}{\partial m}+\frac{1}{2\left(1+\delta_E\right)}\frac{\partial\delta_E}{\partial m}\right)+\frac{\vec{\kappa}}{\kappa}\frac{\partial\vec{U}}{\partial m}\right] \tag{7}$$

The diffraction parameter δ_E is based on a spatial averages of properties of the wave field according to:

$$\delta_E = \frac{\nabla \bullet \left(cc_g \nabla \sqrt{E} \right)}{\kappa^2 cc_g \sqrt{E}}, \tag{8}$$

where c and c_g and the phase and group velocity, respectively. The diffraction parameter δ_E adds a second order spatial derivative to the system of equations.

The SWAN model has a number of switches to control diffraction. Apart from a general switch for turning diffraction on or off, there are two parameters that control the evaluation of the diffraction parameter δ_E; SMPAR and SMNUM. To avoid numerical instabilities in the evaluation of the diffraction parameter, its evaluation is based on a smoothed field of wave energy between neighbouring spatial grid points. The SMPAR parameter controls the amount of smoothing between neighbouring grid points. The parameter SMNUM controls the number of times that a smoothing operation is performed.

Smoothing is performed on the basis of the directionally integrated energy $E(\sigma)$ in neighbouring spatial grid points according to:

$$E_{i,j}^{n} = E_{i,j}^{n-1} - SMPAR \times \left[E_{i-i,j} + E_{i,j-1} - 4E_{i,j} + E_{i+1,j} + E_{i,j+1} \right]^{n-1} \tag{9}$$

The default value of SMPAR is 0.2 (see Eq. 17 in Holthuijsen et al., 2003).

The smoothing of the wave fields is only used for the computation of the diffraction parameter δ_E, it does not affect the wave field as used in the action balance equation.

3. METHODOLOGY AND FUNCTIONALITY TESTS

To evaluate the performance of SWAN with diffraction we consider the simple case of an infinite breakwater in water of constant depth. The advantage of this approach is that numerical solutions can be compared with analytical solutions. If it turns out that diffraction 'works' in SWAN, we plan to investigate more complex cases.

For the present study we consider a rectangular domain with various dimensions. The semi-infinite breakwater is located halfway along the lower boundary pointing upwards. In the SWAN model it is modelled as an obstacle object with zero reflection and zero transmission. Along all up-wave boundaries an incoming wave conditions is prescribed. The basic case is a wave travelling from left to right, with a period (T) of 8 s in water of depth 10 m. Three cases are considered for the short-crestedness of the wave with rms energy weighted spreading of $\sigma = 1.5°$ (uni-directional), $\sigma = 10°$ (swell) and $\sigma = 30°$ (wind waves). The directional spreading is defined according to Kuik et al. (1988).

The performance of diffraction in SWAN was tested in 2 phases. In the first phase we concentrated on the implementation of diffraction in SWAN. To that end the following tests were performed:

- Effect of spatial resolution Δs;
- Effect of the size of the computational domain;
- Effect of smoothing;
- Effect of depth;

In the second phase we concentrated on the validation of the diffraction approximation in SWAN. To that end the following activities were carried out:

- Comparison against an analytical solution;
- Determine the areas where diffraction is important;
- Determine the role of directional spreading on the results;

The entrance boundary condition was specified by a narrow banded Gaussian-shaped frequency spectrum centered on the period of the wave *T*, with a width of 0.01Hz (standard deviation). This condition was applied on the north and west sides, and on the section of the south side ahead of the breakwater.

The directional resolution was kept constant for each of the three main cases. Following guidance from the SWAN manual, we chose for the case $\sigma = 1.5°$, $\Delta\theta = 0.5°$; for $\sigma = 10°$, $\Delta\theta = 2°$; for $\sigma = 30°$, $\Delta\theta = 10°$.

4. RESULTS

4.1 Analytical benchmarks

An analytical solution is available for the wave height and direction that accounts for the diffraction around a semi-infinite breakwater (see Wiegel, 1962). This solution is for regular, unidirectional waves. However, the solution can be extended for short-crested waves (waves with directional spreading) and for irregular waves by using the principle of superposition.

Figures 1 and 2 show the solution obtained using the model for waves with a directional spreading of 1.5° and of 30° respectively for the base case. The results are shown over an area of about 1200 m by 1200 m, (16 by 16 wavelengths). As expected, the wave height variation for the case with 30° of directional spreading is considerably smoother than for the case with 1.5° of spreading. In addition, the area behind the breakwater is less sheltered when the wave field is more directionally spread. In the case with 1.5° of spreading, wave heights up to 1.13 m are found, as expected in the analytical solution.

4.2 Spatial resolution

An early finding was that SWAN computations with diffraction become unstable if the spatial resolution is too fine. Computations were made for the case with 1.5° directional spreading for various wave periods to establish the limits of acceptable spatial resolution. Regardless of the wave period, it was found that computations carried out with 3.5 grid points per wavelength (L) were stable, whereas computations with 4 grid points per wavelength were unstable.

Figures 3 (3.5 grid points per wavelength) and 4 (4 grid points per wavelength) give an example of the results of SWAN computations with diffraction for a computational area of 1000 m by 1000 m for the base case with 1.5° spreading. The results of the instability for the case with 4 grid points per wavelength are clearly visible in the top right hand corner of Figure 4, but also at some points directly behind the breakwater.

The same limits were found for cases with more directional spreading and other water depths.

The effect of the spatial resolution on the accuracy of the results was also tested. Figure 5 shows the difference between the result of SWAN with 3 points per wavelength and the analytical solution for the case with 1.5° of spreading. It can be seen that the results are within 5 cm over the whole area except the area immediately behind the breakwater. Figure 6 shows a similar result for a SWAN computation made with 1 point per wavelength. In this case there are significant areas in which the error is greater than 15 cm and a large area behind the breakwater where the error is greater than 10 cm. Similar but less pronounced results are obtained for the case with 30° directional spreading (see below). We therefore conclude that it is beneficial to use resolution that is as fine as possible given the upper limit of 3.5 grid points per wavelength and possible restrictions on the size of the computational grid (see section 4.3).

4.3 Size of computational area

In SWAN computations with diffraction for a low directional spreading (1.5°) and a fine directional resolution (0.5°), it was found that instabilities occurred if the number of grid points in the computational area is too large. No practical limitation on the grid size was found for cases with directional spreading of 30° or a coarser directional resolution (10°).

Figures 7 and 8 show the results of the SWAN computations for the base case with a grid of 67 points by 67 points (22 wavelengths) and of 79 points by 79 points (26 wavelengths) respectively. In both cases, the spatial resolution was 3 points per wavelength. The effects of the instability can be clearly seen in the top right corner of Figure 8, but not in Figure 7. This result was shown to be independent of the wave period.

We therefore recommend that for computations with diffraction where narrow directional spectra may occur, the size of the computational area be limited to about 65 grid points by 65 grid points.

4.4 The use of smoothing

The use of smoothing makes it possible to obtain stable results with a finer spatial resolution. The accuracy of the results with smoothing (smoothing number = 6, smoothing parameter = 0.2) and a finer resolution (5 grid points per wavelength) was therefore examined for the situation with 1.5° of spreading. Five grid points per wavelength was chosen because this is the best accuracy that can be obtained without instability with this smoothing number.

The results are given in Figure 9, which shows the difference between the results computed by SWAN with smoothing and the analytical solution. This should be compared with Figure 5 in which a resolution of 3 points per wavelength was used without smoothing for the same conditions. It can clearly be seen that the results with smoothing are considerably worse for this situation, particularly in the area directly behind the head of the breakwater.

It is therefore concluded that for incident waves with a small directional spreading it is not worthwhile to use smoothing.

4.5 The requirement to include diffraction

There is often discussion about the need to include diffraction in the computation for situations with short-crested waves. Therefore computations were made with and without diffraction for the base case with directional spreading of 30°. Figure 10 shows the relative difference between the SWAN computation with diffraction (3 grid points per wavelength, diffraction, no smoothing) and the analytical solution. Figure 11 shows the relative difference between the SWAN computation without diffraction (6 grid points per wavelength) and the analytical solution. In general, the solution without diffraction gives better results than the solution with diffraction. In the area immediately behind the breakwater (where the wave height is very low anyway) the result with diffraction is significantly better than the result without diffraction.

Figures 12 and 13 show similar results for the base case with 10° spreading. In this case, it can be seen that the results with diffraction are considerably better than the results without diffraction.

It is therefore concluded that for situations with narrow directional spectra (say, less than 15°), the SWAN model should be used with diffraction. In situations with wide spectra, it seems to be better to use SWAN without diffraction. Further work should be carried out to investigate the effect of directional resolution when diffraction is applied.

5. DISCUSSION

The present study revealed some practical limitations to the use of diffraction for narrow banded frequency waves in the SWAN model. Especially, the limitations on grid resolution and grid size are important for using SWAN with diffraction. In some cases instabilities occur, degrading the results. These instabilities are probably related to the computational method of computing the second order derivatives and they seem to originate at the boundary of the computational domain. Therefore, further work is recommended to improve the numerical treatment of diffraction in SWAN.

The tests for the semi-infinite breakwater revealed that the diffraction approximation works quite well. As expected, the effect of directional spreading is to smooth out the typical spatial variation due to diffraction, since local variations of different spectral component cancel each other. In such cases, it is not needed to turn diffraction on.

Further tests are recommended to assess the performance of diffraction in SWAN. As a first step numerical tests should be performed to assess the effect of broader frequency spectra and the directional resolution on the computational results. An interesting case would be to assess the combined effect of refraction and diffraction in an access channel towards a harbour. Also, verification against two-dimensional phase-resolving models is recommended.

6. CONCLUSIONS

In this study the practical applicability of diffraction in SWAN 40.51 for narrow banded frequency waves was evaluated leading to the following conclusions:

- Stable results can be found when the dimensionless parameter $L/\Delta s$ is smaller than 3.5;
- Stable results can be found when the size of the computational domain is less than 65 by 65 grid points;
- Too much smoothing degrades the results since the diffraction parameter becomes meaningless;
- For the case of a semi-infinite breakwater diffraction is computed reasonably well;
- The effect of directional spreading reduces the importance of diffraction;
- The practical limits are independent of water depth.

It is stressed that the present results are based on SWAN model version 40.51. Since the SWAN model is continuously being developed, it is expected that the source of the observed instabilities will be identified and resolved in future versions of the SWAN model.

REFERENCES

Berkhoff, J.C.W., 1972: Computations of combined refraction-diffraction. Proc. 13th Int. Conf. on Coastal Engineering, 471-478,

Booij, N., L.H. Holthuijsen, and P.H.M. De Lange, 1992: The penetration of short-crested waves through a gap. Proc. 23rd Int. Conf. On Coastal Engineering.

Booij, N., R.C. Ris, and L.H. Holthuijsen, 1999: A third generation wave model for coastal regions. Part I, Model description and validation. J. Geophys. Res., **104**, C4, 7649-7666.

Borsboom, M., N. Doorn, J. Groeneweg, and M. Van Gent, 2000: A Boussinesq-Type wave model that conserves both mass and momentum. Proc. 27th Int. Conf. on Coastal Engineering. 148-161.

Groeneweg, J., N. Doorn, M.J.A. Borsboom, and A.R. Van Dongeren, 2004: Near-shore wave modelling with two coupled models: swan and triton. Proc. 29th Int. Conf. On Coastal Eng., 868-880.

Holthuijsen, L.H., N. Booij, A.T.M.M. Kieftenburg, R.C. Ris., A.J. Van der Westhuysen, and M. Zijlema, 2004: SWAN cycle III, Version 40.41, User manual.

Holthuijsen, L.H., A. Herman, and N. Booij, 2003: Phase-decoupled refraction-diffraction for spectral wave models. Coastal Engineering, **49**, 291-305.

Kuik, A.J., G.Ph. van Vledder, and L.H. Holthuijsen, 1988: A method for the routine analysis of pitch-and-roll buoy wave data. J. Phys. Oceanogr., **18**, 1020-1034.

Rivero, F.J., A.S. Arcilla, and E. Carci, 1997: Analysis of diffraction in spectral wave models. Proc. 3rd Int. Symp. Ocean Wave Measurement and Analysis, WAVES '97, ASCE, New York, 431-445.

Wiegel, R.L., 1962: Diffraction of Waves by a Semi-infinite Breakwater. Journal of the Hydraulics Division, **88**, No. HY1, Jan. 1962, pp 27-44.

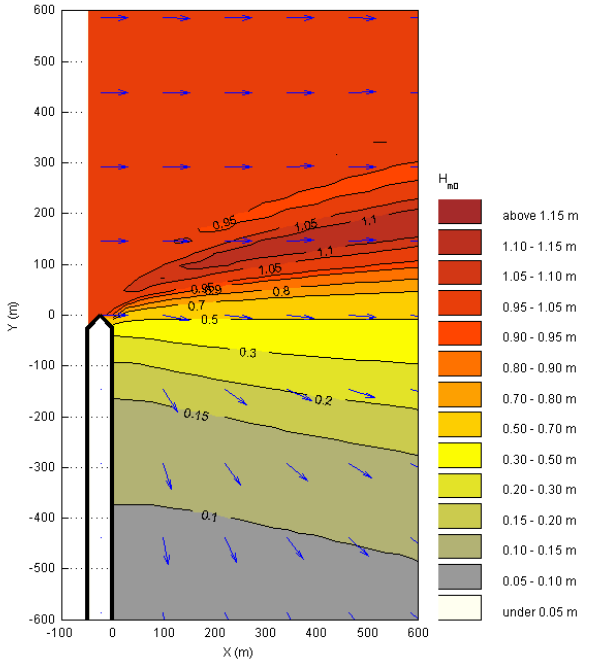

Figure 1: Spatial variation of significant wave height behind a semi-infinite breakwater based on an analytical solution. Incident wave conditions: H = 1.0 m, T = 8 s, θ = 0° and σ = 1.5°.

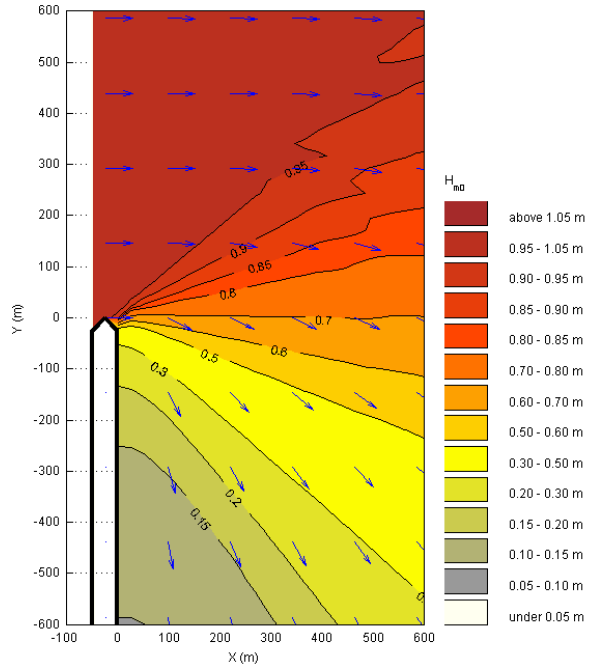

Figure 2: Spatial variation of significant wave height behind a semi-infinite breakwater based on an analytical solution. Incident wave conditions: H=1.0 m, T = 8 s, θ= 0° and σ=30°.

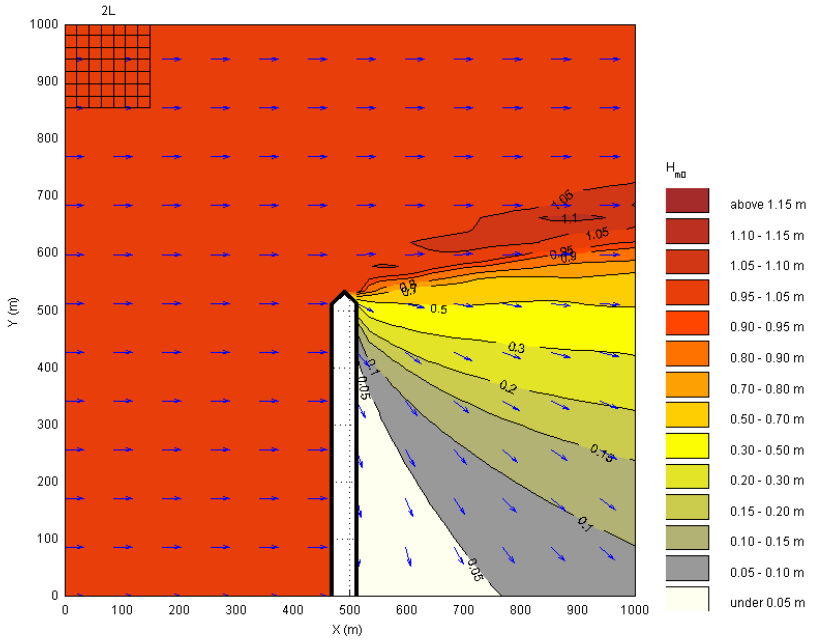

Figure 3: Spatial variation of significant wave height behind a semi-infinite breakwater from a SWAN computation with diffraction. Resolution $L/\Delta s$=3.5. Depth = 11 m. Incident wave conditions: H_{m0}=1.0 m, T = 8 s, θ=0° and σ=1.5° (NW corner: sample of the mesh over area 2L×2L).

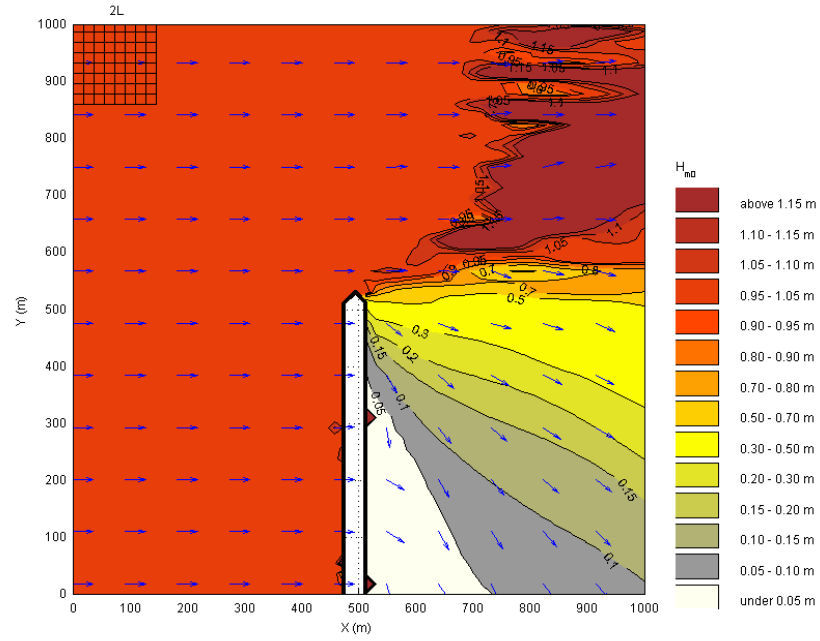

Figure 4: Spatial variation of significant wave height behind a semi-infinite breakwater from a swan computation with diffraction. Resolution L/Δs=4. Depth = 11m. Incident wave conditions: Hm0=1.0m, T = 8s, θ=0° and σ=1.5°. (NW corner: sample of the mesh over area 2L×2L).

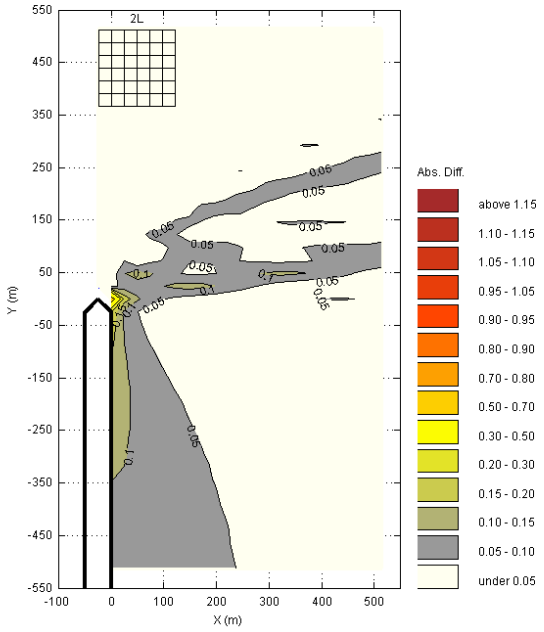

Figure 5: Spatial variation of difference between significant wave height predicted by swan with diffraction and analytical solution (Hswan – Hanal). Swan resolution L/Δs=3.0. Depth = 11m. Incident wave conditions: Hm0=1.0m, T = 8 s, θ = 0°, σ=1.5 and Δθ = 0.5°. (NW corner: sample of the mesh over area 2L×2L).

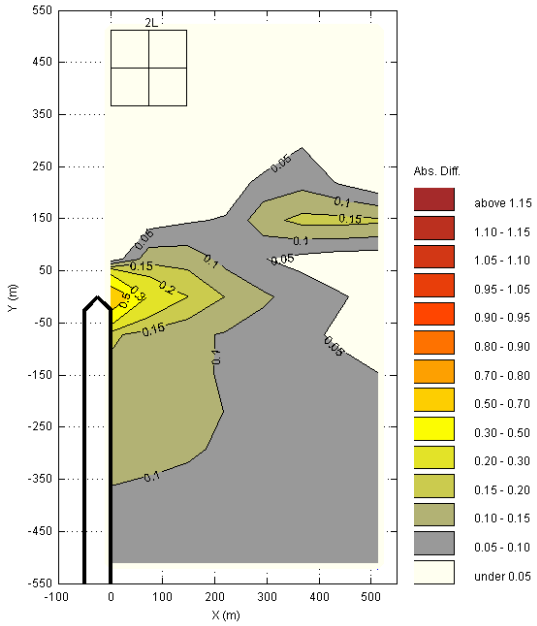

Figure 6: Spatial variation of difference between significant wave height predicted by swan with diffraction and analytical solution (Hswan – Hanal). Swan resolution L/Δs=1.0. Depth = 11 m. Incident wave conditions Hm0=1.0 m,T = 8 s, θ=0°, σ=1.5 and Δθ = 0.5°. (NW corner: sample of the mesh over area 2L×2L).

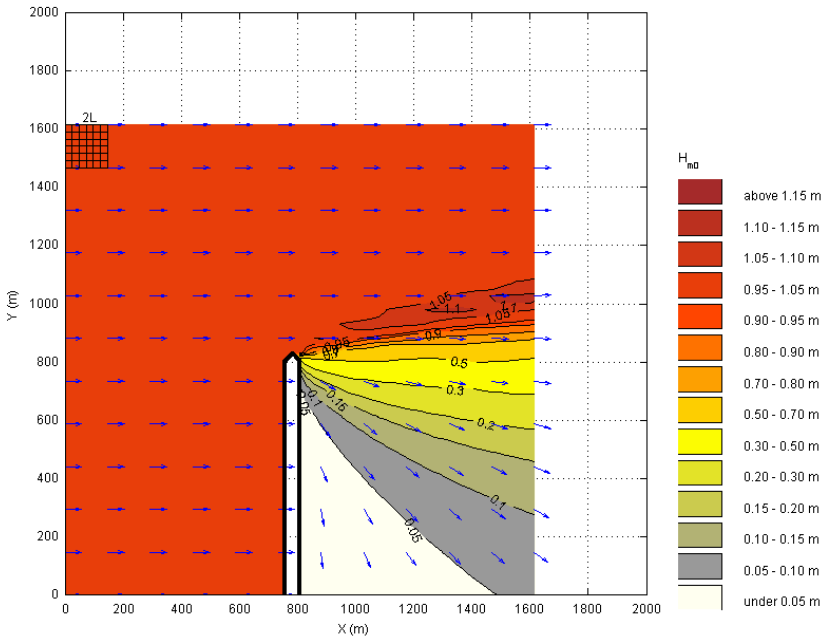

Figure 7: Spatial variation of the significant wave height behind a semi-infinite breakwater from a SWAN computation with diffraction. Resolution $L/\Delta s=3$. Grid size 22 by 22 wavelengths. Depth = 11 m. Wave period T=8 s, H_{m0}=1 m, θ=0°, σ=1.5° and $\Delta\theta$=0.5°. (NW corner: sample of the mesh over area 2L×2L).

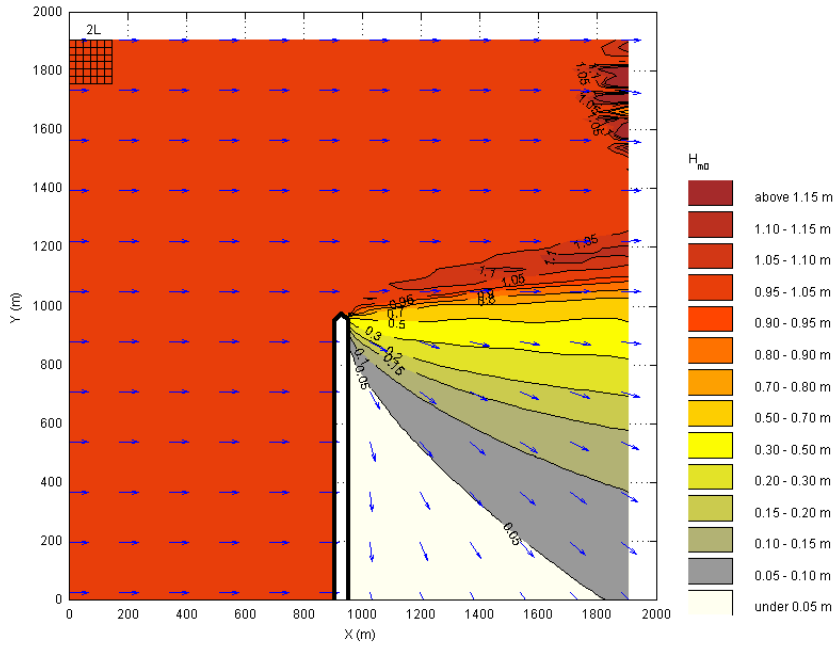

Figure 8: Spatial variation of the significant wave height behind a semi-infinite breakwater from a SWAN computation with diffraction. Resolution $L/\Delta s=3$. Grid size 26 by 26 wavelengths. Depth = 11m. Wave period T= 8 s, H_{m0}=1 m, θ=0°, σ=1.5°, $\Delta\theta$=0.5°. (NW corner: sample of the mesh over area 2L×2L).

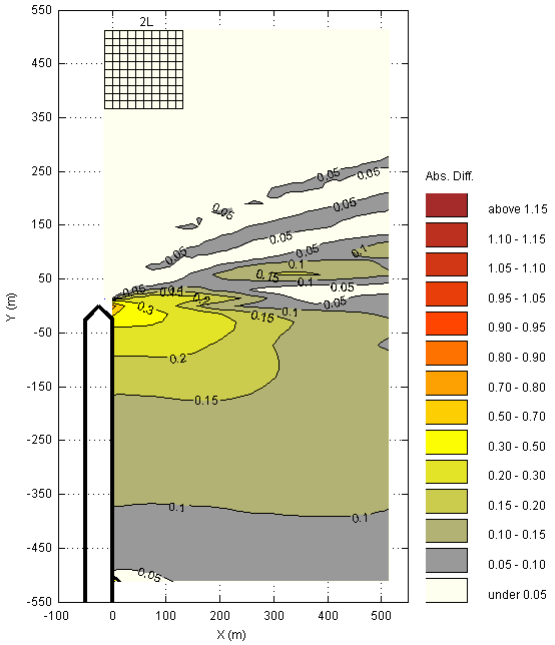

Figure 9: As in Figure 5, but with a spatial resolution of $L/\Delta s$=5 and smoothing number SMNUM=6. (NW corner: sample of the mesh over area 2L×2L).

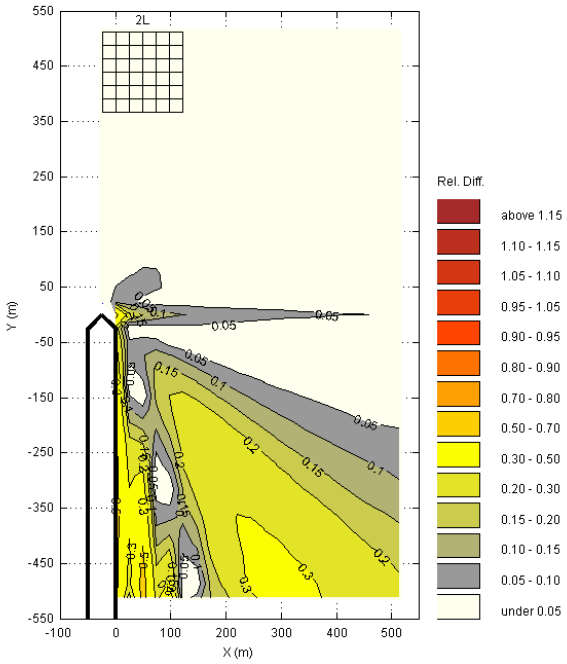

Figure 10: Spatial variation of relative difference between wave height predicted by SWAN with diffraction and analytical solution (H_{SWAN}-H_{ANAL})/H_{ANAL}. Resolution L/Δs=3. Depth = 11m. Incident wave conditions: H_{m0}=1.0 m, T = 8 s, θ=0°, σ=30° and $\Delta\theta$ = 10°. (NW corner: sample of the mesh over area 2L×2L).

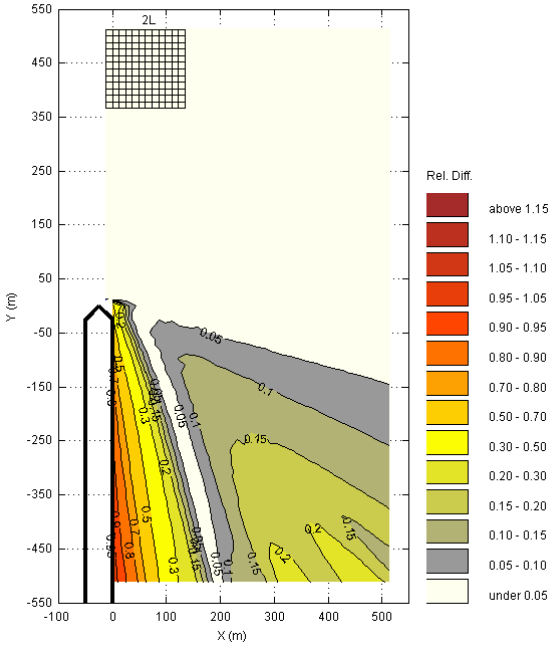

Figure 11: Spatial variation of relative difference between wave height predicted by swan without diffraction and analytical solution (H_{SWAN}-H_{ANAL})/H_{ANAL}. Resolution $L/\Delta s$=6. Depth = 11m. Incident wave conditions: H_{m0}=1.0 m, T = 8 s, θ=0°, σ=30° and $\Delta\theta$ = 10°. (NW corner: sample of the mesh over area 2L×2L).

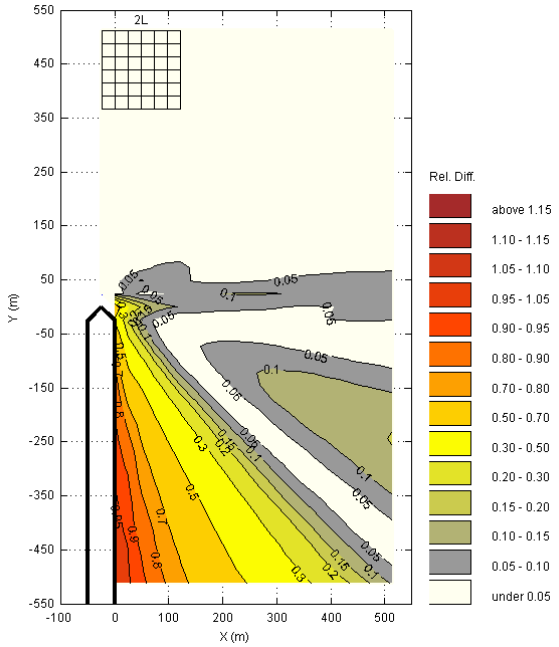

Figure 12: Spatial variation of relative difference between wave height predicted by SWAN with diffraction and analytical solution (H_{SWAN}-H_{ANAL})/H_{ANAL}. Resolution $L/\Delta s$=3. Depth = 11m. Incident wave conditions: H_{m0}=1.0 m, T = 8 s, θ=0°, σ=10° and $\Delta\theta$ = 2°. (NW corner: sample of the mesh over area 2L×2L).

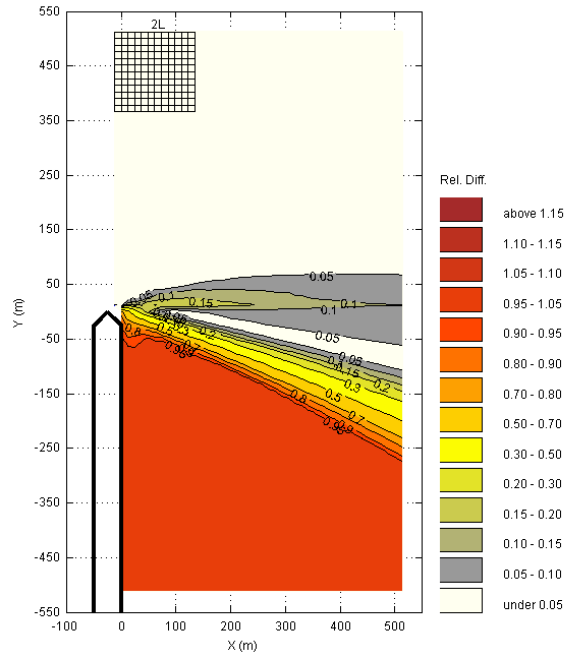

Figure 13: Spatial variation of relative difference between wave height predicted by SWAN without diffraction and analytical solution (H_{SWAN}-H_{ANAL})/H_{ANAL}. Resolution $L/\Delta s$=6. Depth = 11m. Incident wave conditions: H_{m0}=1.0 m, T = 8 s, θ=0°, σ=10° and $\Delta\theta$ = 2°. (NW corner: sample of the mesh over area 2L×2L).